ELSEVIER

Thermochimica Acta 314 (1998) 131–136

thermochimica acta

Thermodynamic properties of Cobalt–Praseodymium alloys

S Bär, H.-J. Schaller*

Institut für Physikalische Chemie der Universität Kiel, Olshausenstr. 40, D-24118 Kiel, Germany

Received 26 September 1997; accepted 27 October 1997

Abstract

The thermodynamic properties of Co–Pr alloys have been determined between 973 and 1073 K by electromotive force measurements on galvanic cells employing CaF_2 as a solid electrolyte. Results yield a complete set of thermodynamic functions for the intermetallic phases (Co), $Co_{17}Pr_2$, Co_5Pr, Co_7Pr_2, Co_3Pr, and Co_2Pr which are compared with data for analogous alloys available from the literature and with predicted values from the Miedema model. The influence of the electronic structure of the components on the energetics of alloy formation is discussed. © 1998 Elsevier Science B.V.

Keywords: Alloys; Thermodynamics; Phase Equilibria; EMF

1. Introduction

Intermetallic compounds formed between rare-earth elements (R) and 3d metals have attracted much recent attention of their interesting physical and thermochemical properties and because of their technological importance. Compounds which occur in the R–Fe and R–Co systems find practical application as starting materials for the manufacture of novel permanent magnets offering outstanding hard magnetic properties. The knowledge of the phase diagrams and of the thermodynamic properties of these systems is essential for improving the metallurgical processes involved in the manufacture of the magnets and for predicting the stability and behaviour in the case of practical application.

Phase diagrams for the Pr–Co systems have been proposed by Ray [1] with nine intermetallic compounds and more recently by Wu et al. [2] with eight intermetallic compounds. The results of these studies are mostly in good agreement except for the type of melting of $Co_{17}Pr_2$ and the presence or absence of the Co_2Pr phase as reported by Ray. The Co–Pr phase diagram most recently assessed by Okamoto [3] is based primarily on the work of Wu et al. with modifications concerning the phase $Co_{19}Pr_5$ and Co_2Pr_5. The ranges of stability of $Co_{19}Pr_5$ and Co_7Pr_2 were reported by Wu et al. to extend from 400°C up to the melting points at 1120 and 1130°C, respectively. According to Okamoto, it is unlikely that two compounds with very similar compositions exist in a wide temperature range; therefore $Co_{19}Pr_5$ was assumed to be a high temperature phase such as the analogous compound $Co_{19}Sm_5$. Except for the heat of formation of the intermetallic compound Co_2Pr [4], thermodynamic information on the Co–Pr system is not available.

The purpose of the present paper is to provide a complete set of thermodynamic functions for Co–Pr alloys and to check the phase relations.

*Corresponding author.

PII S0040-6031(97)00461-9

2. Experimental

Emf measurements on galvanic cells with CaF_2 solid electrolytes have turned out to be a reliable method to determine the thermodynamic properties of alloys containing a strongly electropositive component such as an rare earth metal. The Co–Pr system was studied between 973 and 1073 K by operating cells of the following type:

$$\mathrm{Ta|Pr, PrF_3|CaF_2|Co - Pr(alloy), PrF_3|Ta} \quad \text{(I)}$$

Single crystals of CaF_2 (Kohrt), approximately 2.5 mm thick and 1 cm in diameter, were used as solid electrolytes. Even under the strongly reducing conditions pregiven by the equilibrium of the Pr, PrF_3 electrode, CaF_2 exhibits pure ionic conductivity. Tantalum foils turned out to be suitable electrical contacts for the electrodes in cell (I).

Provided cell (I) is operating reversibly, the electromotive force E is directly related to the activity a_{Pr} of Pr in the alloy without the use of any auxiliary data:

$$E = -\frac{RT}{3F}\ln a_{Pr} \quad (1)$$

The alloys were prepared from weighed amounts of Pr (99.9%, Heraeus) and Co (99%, Heraeus) by induction melting in a water cooled copper boat under a flow of purified argon. Homogenization of the alloys was achieved by successively inverting and remelting the specimens several times followed by a heat treatment under a continuous flow of argon between 1073 and 1173 K for 14 days. The formation of the phases was checked by X-ray measurements. Alloys were stored and handled under argon. Fine particles were produced from the non-brittle alloys by grinding with a tungsten carbide drill and from the brittle alloys by crushing in a mortar. The powder was then mixed with about 20 wt.% PrF_3 powder (99.9 Heraeus) and pressed into tablets, approximately 1 mm thick and 7 mm in diameter.

Details of the experimental arrangements are given in a previous paper [5]. After the assembly of the cell, the apparatus was successively evacuated and filled with argon several times. The cells were then heated to 473 K, and maintained at that temperature under vacuum for 1 h. A slow flow of argon was then established which was maintained during the experiment. Before entering the cell assembly, argon was passed through dry $Mg(ClO_4)_2$ at room temperature and over zirconium turnings at 1273 K to eliminate traces of water and oxygen, respectively. In previous investigations this method of purification has turned out to be very effective. The emf was measured with a digital voltmeter (input impedance $> 10^9\ \Omega$). The experiment was completely controlled by a computer which helped to increase the number of recorded data points and to improve the accuracy. After heating the cells to 1073 K a period of 12 h was allowed for initial equilibration of the emf. Temperature and emf were recorded after reaching values constant within ± 1 K and ± 0.3 mV, respectively. Subsequently, the temperatures of measurements were successively approached from above and below, and stable emf values were attained in typically 2 to 3 h after thermal equilibrium. The observed absence of a hysteresis of the recorded emf data indicates the thermal reversibility of the operated cells. As a further test of reversibility, a small current was passed for a short time through the cell in either direction. After the imposed perturbation was removed, the open-circuit emf returned to its original value in a short time (typically 5 to 15 min).

3. Results

Seventeen Co–Pr alloys containing 3.3 to 40.0 at % Pr were investigated between 973 and 1073 K. In each of the computer-controlled experiments 20 emf data were recorded in this temperature range; two experimental runs were made with each alloy. As checked by running independent cells, the electromotive force values were reproducible within ± 0.5 mV.

The results of the emf measurements on cell (I) as obtained from least-squares fits are listed in Table 1.

The activities of Pr in Co at 973, 1023 and 1073 K calculated from Eq. (1) are plotted vs. composition in Fig. 1. The terminal solid solubility of Pr in Co was reported by Wu et al. [2] to be about 0.03 at % Pr. Since the phases have quite narrow ranges of homogeneity between 1073 and 1173 K [3], they are assumed to be line compounds.

Considering the negligible ranges of homogeneity, the virtual cell reactions occurring in cell (I) upon the passage of three Faraday may be formulated as follows:

Table 1
Results of the electromotive force measurements between 973 and 1073 K on galvanic cells of the type: Pr, $PrF_3|CaF_2|Co-Pr, PrF_3$

Phases	Electromotive force E at 1073 K in mV	dE/dT in mV/k
(Co)+$Co_{17}Pr_2$	224.1	0.0280
$Co_{17}Pr_2$+Co_5Pr	170.1	0.0337
Co_5Pr+Co_7Pr_2	148.7	−0.0956
Co_7Pr_2+Co_3Pr	125.4	−0.0570
Co_3Pr+Co_2Pr	82.3	−0.0200
Co_2Pr+liquid	28.9	−0.1125

$$3F: \frac{17}{2}Co + Pr = \frac{1}{2}Co_{17}Pr_2,\ \Delta_r G_1 \quad (2)$$

$$3F: \frac{5}{7}Co_{17}Pr_2 + Pr = \frac{17}{7}Co_5Pr,\ \Delta_r G_2 \quad (3)$$

$$3F: \frac{7}{3}Co_5Pr + Pr = \frac{5}{3}Co_7Pr_2,\ \Delta_r G_3 \quad (4)$$

$$3F: 3Co_7Pr_2 + Pr = 7Co_3Pr,\ \Delta_r G_4 \quad (5)$$

$$3F: 2Co_3Pr + Pr = 3Co_2Pr,\ \Delta_r G_5 \quad (6)$$

The free enthalpies of reaction $\Delta_r G_i$ (i=1···5) are given by $\Delta_r G_i = -3FE_i$, where E_i are the electromotive forces measured in the corresponding two phase fields (see Table 1). The free enthalpies of formation of the intermetallic compounds $\Delta G_f(Co_xPr_y)$ may be calculated by means of following expressions:

$$\Delta G_f(Co_{17}Pr_2) = -6F \cdot E_1 \quad (7)$$

$$\Delta G_f(Co_5Pr) = -\frac{21}{17}F \cdot E_2 + \frac{5}{17}\Delta G_f(Co_{17}Pr_2) \quad (8)$$

$$\Delta G_f(Co_7Pr_2) = -\frac{9}{5}F \cdot E_3 + \frac{7}{5}\Delta G_f(Co_5Pr) \quad (9)$$

$$\Delta G_f(Co_3Pr) = -\frac{3}{7}F \cdot E_4 + \frac{3}{7}\Delta G_f(Co_7Pr_2) \quad (10)$$

$$\Delta G_f(Co_2Pr) = -F \cdot E_5 + \frac{2}{3}\Delta G_f(Co_3Pr) \quad (11)$$

The corresponding entropies of formation $\Delta S_f(Co_xPr_y) = -\left(\frac{\delta \Delta G_f}{\delta T}\right)$ may be calculated from the temperature dependence $\left(\frac{\delta \Delta E_i}{\delta T}\right)$ listed in Table 1.

The thermodynamic functions for the formation of Co_xPr_y intermetallic compounds, the free enthalpies of formation ΔG_f at 1073 K and the enthalpies ΔH_f and ΔS_f which represent mean values determined between 973 and 1073 K are tabulated on a per mole of atoms base

$$\Delta Y_f = \frac{1}{x+y}\Delta Y_f(Co_xPr_y),$$

Y=G, H and S in Table 2.

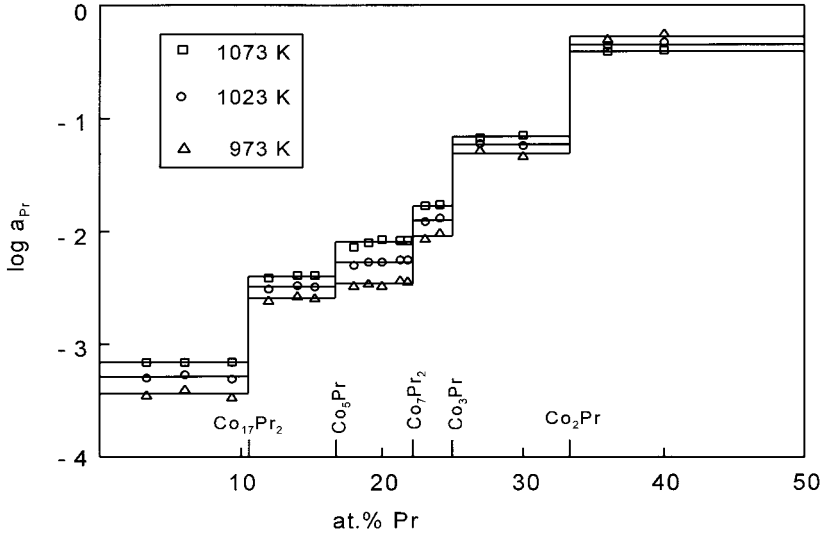

Fig. 1. Activity of Pr in Co–Pr alloys (reference state: Pr solid).

Table 2
Integral thermodynamic functions of Co_xPr_y alloys: free enthalpy of formation ΔG_f at 1073 K and mean values for the enthalpies ΔH_f and entropies ΔS_f in the temperature range 973 to 1073 K

Phase	ΔG_f in kJ/mol atoms	ΔH_f in kJ/mol atoms	ΔS_f in kJ/kmol atoms
$Co_{17}Pr_2$	−6.83	−5.91	0.85
Co_5Pr	−9.74	−8.17	1.46
Co_7Pr_2	−11.96	−12.47	−0.48
Co_3Pr	−12.83	−13.96	−1.05
Co_2Pr	−14.05	−15.74	−1.58

4. Discussion

Since the activity of a component in an alloy is constant in two phase fields and increases with composition in single phase fields, the determination of activity isotherms contribute to clarify phase relations. The activity isotherms in Fig. 1 indicate the existence of the following compounds in the temperature range between 973 and 1073 K: $Co_{17}Pr_2$, Co_5Pr, Co_7Pr_2, Co_3Pr, and Co_2Pr. Co_5Pr was supposed to decompose in an eutectoidic reaction in the adjacent phases [6]. Since the activity isotherms confirm the existence of this compound, the decomposition should occur below 973 K. Since the activity of Pr is constant in the Co_5Pr–Co_7Pr_2 two phase field $Co_{19}Pr_2$ is not stable in the temperature range of the present measurements. This finding is in accordance with the above mentioned suggestion of Okamoto that $Co_{19}Pr_2$ is stable at high temperatures only.

Wu et al. [2] have reported the solid solubility of Pr in α - Co to be about 0.03 at. % Pr at 1273 K. X-ray measurements made in the present study on a number of two-phase alloys with small Pr contents (up to 1.5 at. % Pr) yielded an expansion of the lattice of α - Co by 0.04 pm upon alloying with Pr.

Using this information, the partial molar volume of Pr is estimated to be $(14.3\pm2)\cdot10^{-6}$ m^3/mol. This value is considerably larger than the molar volume of Co ($6.7\cdot10^{-6}$ m^3/mol). The large volume difference is considered to be the factor mainly responsible for the low solid solubility of Pr in Co.

The activities of Pr in the solid solution range show small deviations from Raoult's law. Using the activity data in the (Co)+$Co_{17}Pr_2$ two-phase field and the solubility limit of 0.03 at. % reported by Wu et al., [2] the relative partial excess Gibbs energy of Pr in the (Co) solid solution, $\Delta\bar{G}^E_{Pr} = RT(\ln a_{Pr} - \ln x_{Pr})$, was calculated to be 7±4 kJ/mol at 1073 K.

Following an analysis carried out for a number of analogous solid solution alloys [6–12], two opposing effects are considered to be responsible for the deviations from ideality. An electronic effect is attributed to a transfer of valence electrons from the Fermi level of Pr to the Fermi level of Co. The charge transfer gives rise to a bonding or electronic (superscript: "e") contribution $\Delta\bar{G}^{Ee}_{Pr}$ to the excess function $\Delta\bar{G}^E_{Pr}$. The elastic effect in solid solution alloys is brought about by the size difference of the components which gives rise to an elastic or dilatational (superscript: "d") contribution $\Delta\bar{G}^{Ed}_{Pr}$. Neglecting an interrelation of both effects, the excess function can be separated in its elastic and electronic part

$$\Delta\bar{G}^E_{Pr} = \Delta\bar{G}^{Ee}_{Pr} + \Delta\bar{G}^{Ed}_{Pr} \tag{12}$$

The following equation, which is based on a simple elastic model [5,7], may be applied in order to determine the elastic part of the excess function at infinite dilution ($X_{pr} = 0$) independent of thermodynamic information:

$$\Delta\bar{G}^{Ed}_{Pr}(x_{Pr} = 0) = \frac{(\bar{V}_{pr} - V_{Co})}{b_{Co}} - \frac{V_{Co}B_{Co}}{b_{Co}(1 - b_{Co})} \times \left(\frac{\bar{V}_{Pr}}{V_{Co}}\right)^{1-b_{Co}} \tag{13}$$

where $\bar{V}_{Pr}$ is the partial molar volume of the solute at infinite dilution, V_{Co} the molar volume of the host metal, B_{Co} the bulk modules at 1 bar, and b_{Co} its pressure coefficient $\left(\frac{\delta B_{Co}}{\delta p}\right)_T$. The $\Delta\bar{G}^{Ed}_{Pr}$ values calculated from Eq. (13) with $B_{Co} = 1.8799\cdot10^{11}$ N/m^2 and $b_{Co} = 2.3305$ [8] are listed in Table 3 together with the experimentally determined value $\Delta\bar{G}^E_{Pr}$ and its electronic part $\Delta\bar{G}^{Ee}_{Pr}$.

Table 3
Relative partial excess free energies with elastic and electronic parts at 1073 K (values refer to infinite dilution)

System	$\Delta\bar{G}^E_i$ in kJ/mol	$\Delta\bar{G}^{Ed}_i$ in kJ/mol	$\Delta\bar{G}^{Ee}_i$ in kJ/mol
Co–Pr	7±4	353±130	−346±134
Co–Al [8]	−159±2	18±4	−177±6
Fe–Pr [9]	41±3	174±16	−133±19
Fe–Al [10]	−72±4	11±3	−83±7

The separation of the excess function illustrates that elastic and electronic interactions exert a strong influence on the thermodynamics of alloying. However, the two opposing effects almost balance each other, and so it happens that the system shows only moderate deviations from ideality.

In previous investigations an analogous analysis was carried out on Co–Al [9], Fe–Pr [10], and Fe–Al [11] alloys. The results are included in Table 3 for comparison.

The partial molar volume of Al dissolved in α - Co (7.6×10^{-6} m^3/mol) is close to the molar volume of the host metal (6.7×10^{-6} m^3/mol). Therefore, $\Delta\bar{G}^{Ed}_{Al}$ has a distinctly smaller value compared to $\Delta\bar{G}^{Ed}_{Pr}$. Since the electronic contribution dominates the mixing behavior of these solid solution alloys, $\Delta\bar{G}^{E}_{Al}$ assumes a pronounced negative value.

As indicated by the data in Table 3, a similar trend shows up for Pr and Al dissolved in Fe as the host metal.

The present experimental values for the Gibbs energy of formation of the intermetallic compounds are shown graphically in Fig. 2 along with the corresponding values for the Fe–Pr [10], Fe–Nd [11], Fe–Y [12], Fe–Th [13], Co–Y [14], Co–Th [15], Ni–Y [16], and Ni–Th [17] systems.

For each system, the Gibbs energies of the compounds are connected by dashed lines. Three trends may be readily recognized from Fig. 2. First, compared to Fe, Co and Ni show a much stronger tendency to form compounds with rare earth metals. Second, the Gibbs energies of formation become more negative in the progression from Fe to Co to Ni. Third, the Gibbs energies of the Th compounds are always distinctly more negative than the corresponding data of the analogous compounds containing Nd, Pr, or Y. Other rare earth metals dissolved in these transition metals in the trivalent state exhibit a similar behavior.

As in the case of the solid solution alloys discussed above, the observed trends in the thermodynamic stability of the alloys may be explained by assuming that the electropositive component behave as electron donors and donate their valence electrons to the electron gas of the alloy. The energy effects resulting from the charge transfer are expected to be determined by the relative position of the Fermi levels of the components and by the valence of the donor metal. The use of the work function as a measure of the Fermi energy shows that the difference in the Fermi levels of

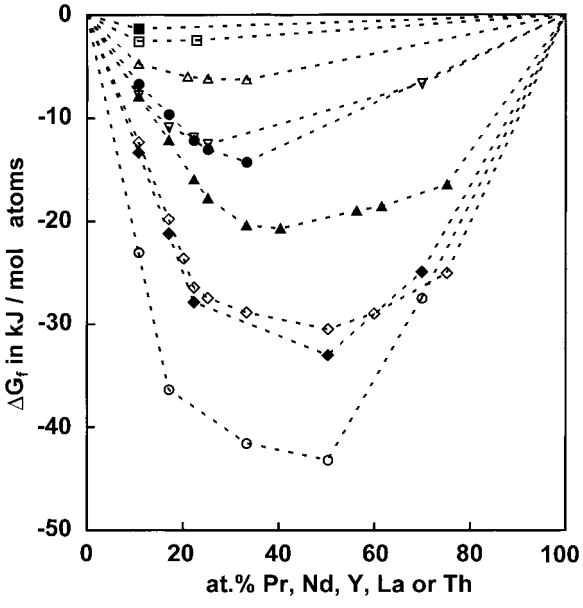

Fig. 2. Gibbs energies of formation for the following alloys as a function of composition at 1073 K: ■ Fe–Pr [10], □Fe–Nd [11], △ Fe–Y [12], ▽ Fe–Th [13], ● Co–Pr (present work), ▲ Co–Y [14], ◆ Co–Th [15], ◇ Ni–Y [16], ○ Ni–Th [17].

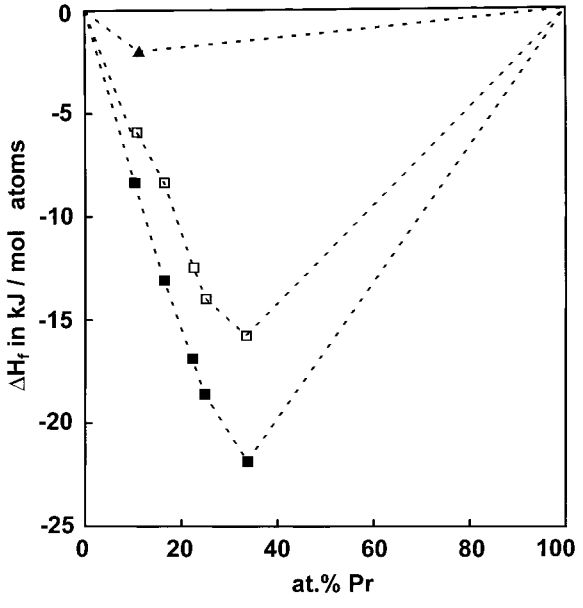

Fig. 3. Enthalpies of formation of Fe–Pr and Co–Pr alloys: ▲ Fe–Pr [10], □ Co–Pr (present work), ■ Co–Pr (predictions of the Miedema model).

the components increases by proceeding from Fe to Co to Ni which explains the second trend described above. The third trend may be attributed to the valence states of electropositive components in the compounds which is three in the case of Nd, Pr and Y and four in the case of Th.

The heats of formation of the intermetallic compounds of the Co–Pr system calculated from the emf data and their temperature dependence are shown in Fig. 3 along with a corresponding value for the $Fe_{17}Pr_2$ compound obtained in a previous emf study [10]. The heat of formation of $Co_{17}Pr_2$ is distinctly more exothermic compared to the corresponding value of $Fe_{17}Pr_2$ .The predicted values of the enthalpies of formation of Co–Pr compounds were calculated using the semi-empirical model of Miedema and coworkers [18] using the most recent sets of parameters [19]. The results are also shown in Fig. 3 for comparison.

From Fig. 3, we see that the Miedema model yields more exothermic values than determined experimentally in all cases. Considering the uncertainties involved, the Miedema predictions are acceptable approximations to the experimental values.

Acknowledgements

Financial support of this work by the Deutsche Forschungsgemeinschaft (DFG) is gratefully acknowledged.

References

[1] A.E. Ray, Cobalt 1 (1974) 3.
[2] C.H. Wu, Y.C. Chuang, X.M. Zin, X.H. Guan, Z. Metallkd. 83 (1992) 32.
[3] H. Okamoto, J. Phase Equil. 13 (1992) 675.
[4] S.S. Deodhar, P.J. Ficarola, Met. Trans. 6A (1975) 1909.
[5] H.-J. Schaller, Ber. Bunsenges. Phys. Chem. 87 (1983) 812.
[6] K.H.J. Buschow, J. Less-Common Met. 29 (1973) 283.
[7] Th. Bretschneider, H.-J. Schaller, Ber. Bunsenges. Phys. Chem. 94 (1990) 185.
[8] Landolt-Börnstein, Tabellen und Funktionen, Springer, Berlin, 6. Auflage, 2. Band 1971, 1. Teil.
[9] H.-J. Schaller, Th. Bretschneider, Z. Metallkd. 76 (1985) 143.
[10] S. Bär, H.-J. Schaller, Z. Metallkd. 86 (1995) 388.
[11] K. Hennemann, H.L. Lukas, H.-J. Schaller, Z. Metallkd. 84 (1993) 668.
[12] P.R. Subramanian, J.F. Smith, CALPHAD 8 (1984) 295.
[13] W.H. Shelton, N.J. Magnani, J.F. Smith, Met. Trans. 4 (1973) 917.
[14] P.R. Subramanian, J.F. Smith, Met. Trans. 16(A) (1985) 1195.
[15] W.H. Shelton, N.J. Magnani, J.F. Smith, Met. Trans. 2 (1971) 473.
[16] P.R. Subramanian, J.F. Smith, Met. Trans. 16B (1985) 557.
[17] W.H. Shelton, N.J. Magnani, J.F. Smith, Met. Trans. 1 (1970) 1833.
[18] A.R. Miedema, P.F. de Chatel, F.R. de Boer, Physica B 100(B) (1980) 1.
[19] A.R. Miedema, A.K. Niessen, Cohesion in metals-transition metal alloys, Philips Research Lab., Eindhoven, 1987.